Cell Reports
Medicine

Report

An mRNA-based platform for the delivery of pathogen-specific IgA into mucosal secretions

Graphical abstract

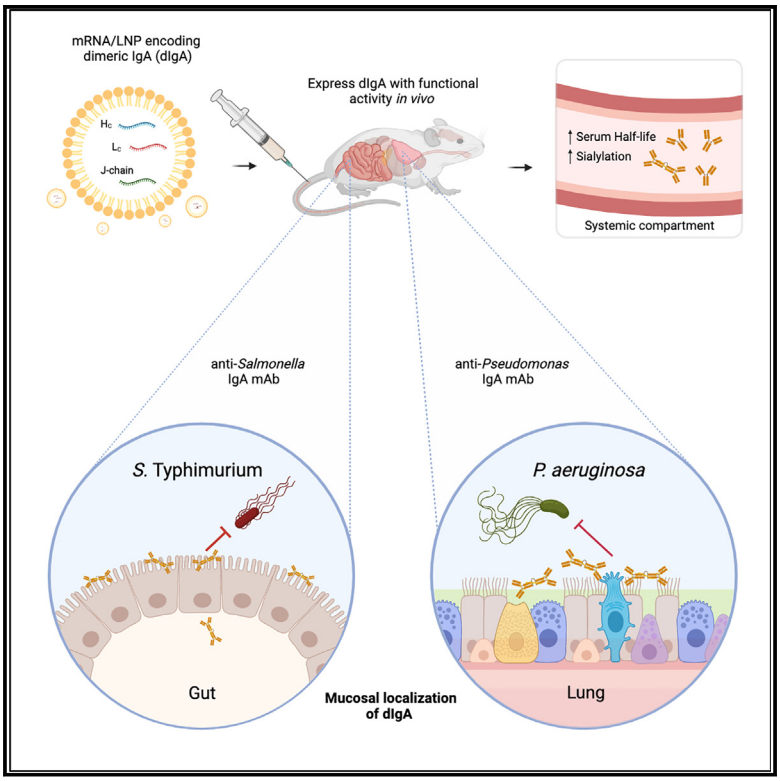

Highlights

- Synthetic mRNAs encoding IgA heavy (H_C), light (L_C), and J chains express dimeric IgA
- *In vivo* mucosal localization of IgA delivered by synthetic mRNA/LNP
- Higher sialylation and serum half-life with IgA from mRNA/LNP than recombinant protein
- Anti-*Salmonella* IgA mAb from mRNA/LNPs reduced invasion during *in vivo* challenge

Authors

Cailin E. Deal, Angelene F. Richards, Tracy Yeung, ..., Nicholas J. Mantis, Andrea Carfi, Obadiah J. Plante

Correspondence

cailin.deal@modernatx.com (C.E.D.), andrea.carfi@modernatx.com (A.C.), obadiah.plante@modernatx.com (O.J.P.)

In brief

Deal et al. report that mRNA/LNPs encoding IgA heavy, light, and J chains express glycosylated dimeric IgA that localizes to mucosal secretions and has a greater serum half-life over recombinant IgA. mRNA-expressed pathogen-specific IgA mAbs limited *Salmonella* Peyer's patch invasion and reduced mortality from *Pseudomonas* acute lung pneumonia in mouse models.

Deal et al., 2023, Cell Reports Medicine *4*, 101253
November 21, 2023
https://doi.org/10.1016/j.xcrm.2023.101253

CellPress

Cell Reports Medicine

CellPress
OPEN ACCESS

Report

An mRNA-based platform for the delivery of pathogen-specific IgA into mucosal secretions

Cailin E. Deal,[1,5,*] Angelene F. Richards,[1] Tracy Yeung,[1] Max J. Maron,[1] Ziqiu Wang,[1] Yen-Ting Lai,[1] Brian R. Fritz,[1] Sunny Himansu,[1] Elisabeth Narayanan,[1] Ding Liu,[1] Rositsa Koleva,[1] Stuart Licht,[1] Chiaowen J. Hsiao,[1] Ivana L. Rajlic,[1] Hillary Koch,[1] Michael Kleyman,[1] Mark E. Pulse,[2] William J. Weiss,[2] Jennifer E. Doering,[3] Samantha K. Lindberg,[4] Nicholas J. Mantis,[3,4] Andrea Carfi,[1,*] and Obadiah J. Plante[1,*]

[1]Moderna, Inc., Cambridge, MA 02139, USA
[2]HSC College of Pharmacy, University of North Texas, Fort Worth, TX 76132, USA
[3]Division of Infectious Diseases, Wadsworth Center, New York State Department of Health, Albany, NY 12211, USA
[4]Department of Biomedical Sciences, University at Albany School of Public Health, Rensselaer, NY 12144, USA
[5]Lead contact
*Correspondence: cailin.deal@modernatx.com (C.E.D.), andrea.carfi@modernatx.com (A.C.), obadiah.plante@modernatx.com (O.J.P.)
https://doi.org/10.1016/j.xcrm.2023.101253

SUMMARY

Colonization of the gut and airways by pathogenic bacteria can lead to local tissue destruction and life-threatening systemic infections, especially in immunologically compromised individuals. Here, we describe an mRNA-based platform enabling delivery of pathogen-specific immunoglobulin A (IgA) monoclonal antibodies into mucosal secretions. The platform consists of synthetic mRNA encoding IgA heavy, light, and joining (J) chains, packaged in lipid nanoparticles (LNPs) that express glycosylated, dimeric IgA with functional activity *in vitro* and *in vivo*. Importantly, mRNA-derived IgA had a significantly greater serum half-life and a more native glycosylation profile in mice than did a recombinantly produced IgA. Expression of an mRNA encoded *Salmonella*-specific IgA in mice resulted in intestinal localization and limited Peyer's patch invasion. The same mRNA-LNP technology was used to express a *Pseudomonas*-specific IgA that protected from a lung challenge. Leveraging the mRNA antibody technology as a means to intercept bacterial pathogens at mucosal surfaces opens up avenues for prophylactic and therapeutic interventions.

INTRODUCTION

The COVID-19 pandemic revealed the potential of synthetic mRNA-based vaccine technology to combat infectious diseases.[1] An inherent advantage of mRNA as a platform technology over more conventional vaccines is the ability to bypass the need for large-scale protein manufacturing and purification.[2] Rather, difficult-to-manufacture proteins and protein complexes, like the trimeric spike proteins of severe acute respiratory syndrome coronavirus 2 (SARS-CoV-2), are expressed *in situ*. While most attention to date on mRNA technology has focused on vaccines, mRNA-based platforms are amenable to the expression of a wide variety of human immune-associated macromolecules. For example, August and colleagues recently completed a phase I clinical trial to evaluate the safety and pharmacology of a lipid nanoparticle (LNP)-encapsulated mRNA encoding the heavy and light chains of a Chikungunya virus (ChikV)-specific neutralizing monoclonal antibody (mAb).[3] The potential of the mRNA/LNP platform for *in vivo* co-expression of a tripartite cocktail of broadly neutralizing antibodies directed against the HIV-1 envelope protein has also been demonstrated.[4]

Immunoglobulin A (IgA) is the predominant antibody isotype in mucosal secretions of the human gastrointestinal (GI) tract and upper airways, where it functions as a first line of defense against pathogenic and opportunistic bacterial pathogens.[5,6] Humans have two IgA subclasses, IgA1 and IgA2, that differ in hinge length, degrees of O-linked glycosylation,[5] and mucosal localization. IgA-secreting B cells are generated in mucosa-associated lymphoid tissues (MALTs) such as Peyer's patches in the small intestine and adenoids in the upper airways in response to environmental antigens and mucosal pathogens.[7] B cells derived from the MALTs take up residence in mucosal tissues as resident plasma cells that secrete IgA as a dimer ($_{d}$IgA) due to co-expression of joining (J) chains.[8] $_{d}$IgA is actively transported across certain epithelial cell barriers by the polymeric Ig receptor (pIgR) and released into mucosal secretions as secretory IgA (SIgA).[9] Neither IgG nor monomeric IgA ($_{m}$IgA), which is the predominant form of IgA in circulation, are actively transported into mucosal secretions by the pIgR.[10] As such, there exists a distinct compartmentalization between systemic and mucosal antibody pools.

The mucosal surfaces that line the GI tract and the upper airways are constantly exposed to a myriad of resident microbiota, as well as opportunistic and pathogenic bacteria. Foodborne pathogens like *Salmonella enterica* serovar Typhimurium (STm) readily invade intestinal tissues, and while antibiotic treatment can clear STm infections, subpopulations of antibiotic-resistant bacteria may persist.[11,12] Similarly, nosocomial infections like *Pseudomonas aeruginosa* (PA) are notoriously difficult to

eradicate once entrenched in the lung, especially considering the degree of antibiotic resistance that exists in clinical isolates.[13] With that in mind, there is a pressing need for both prophylactic and therapeutic interventions aimed at preventing bacterial pathogens from colonizing vulnerable tissues in the first place, as well as clearing infections once established. IgA is ideally suited to accomplish these tasks, especially if pathogen-specific antibodies can be delivered into mucosal secretions at sufficient concentrations to interfere with the earliest steps in the infection process.

Passive immunization with IgA is not a new concept but one that has proven challenging to implement because of the technical obstacles in producing recombinant IgA (IgA_R) and delivering sufficient quantities to be effective for sustained periods.[14] Moreover, human IgA is heavily glycosylated, which poses challenges from a biopharmaceutical standpoint, as N-glycosylation can influence conformation, thermal stability, folding efficiency, solubility, and susceptibility to proteolytic degradation.[15–18] In addition, IgA_R is intractable for most clinical purposes, as it exhibits a shorter serum half-life than IgG due to its inability to recycle through the neonatal Fc receptor,[19] and displays faster clearance from circulation as compared to endogenous human IgA as a result of incomplete sialylation.[20] Efforts to generate IgG/IgA chimeras with desired Fc receptor interactions, serum half-life, and mucosal delivery are ongoing[21–23] but have not reached clinical-stage readiness.

In this report, we investigated the use of synthetic mRNA for *in vivo* production of structurally and functionally intact human IgA. We employed two monoclonal antibodies (mAbs) that have been extensively characterized as recombinant proteins in mouse models of mucosal challenge. Sal4 is an IgA mAb that recognizes the O5− antigen of lipopolysaccharide from STm[24] and has been shown to reduce invasion of STm into intestinal Peyer's patches when administered passively.[24,25] CAM003 is an IgG1 mAb that binds to PA biofilm component Psl and has demonstrated protection in multiple different PA animal models, including acute lung pneumonia.[26,27] Here, Sal4 and CAM003 heavy chains (HCs), light chains (LCs), and J chains (JCs) were encoded as mRNA as human IgA2 ($IgA2_{mRNA}$) or IgA1 ($IgA1_{mRNA}$), respectively, and were characterized *in vitro* and *in vivo* as compared to analogous IgA_R to assess the potential of the mRNA platform to generate potent and protective mucosal mAbs.

RESULTS

Biophysical, functional, and pharmacokinetic properties of mRNA encoded IgA_2

To explore the potential of synthetic mRNA to encode functional monoclonal IgA, mRNA encoding the STm-specific Sal4 HCs and LCs were packaged in LNPs, with or without mRNA encoding the JC.[24,25] Transfection of EXPI293 cells resulted in $IgA2_{mRNA}$ antibody that recognized STm by enzyme-linked immunosorbent assay (ELISA) to a similar level as $IgA2_R$ (Figure 1A). Sal4 $IgA2_{mRNA}$ transfected with the JC was bound by immobilized pIgR similar to $_dIgA2_R$, confirming the formation of $_dIgA$ from mRNA (Figure 1B). The $_mIgA2_R$ product bound pIgR 10-fold less than $_dIgA2_R$, whereas $_mIgA2_{mRNA}$ had no demonstrable interaction with pIgR. Using size-exclusion chromatography (SEC), we observed that $_dIgA2$ predominated over $_mIgA2$ upon JC co-expression *in vitro* and was distinct from $_mIgA2$ and IgA2 aggregates assembled in the absence of the JC (Figure 1C).[28] Differences in aggregate assembly were especially evident following gel electrophoresis of SEC-separated peaks; whereas $_dIgA2$ exhibited bands at the size of JCs (10–15 kDa), these bands were largely absent from the aggregate peak (Figure 1D). Notably, SEC retention times of the $_dIgA2$ and $_mIgA2$ peaks were nearly identical between $IgA2_{mRNA}$ and $IgA2_R$, further demonstrating the expression of similar products (Figure S1). Negative-stain electron microscopy (EM) images of the $_dIgA2_{mRNA}$ preparations revealed Igs in a tail-to-tail oligomerization configuration identical to that of $_dIgA2_R$, demonstrating the ability of mRNA to encode for oligomeric mAbs (Figures 1E and S1). Finally, the functionality of $IgA2_{mRNA}$ was assessed in an *in vitro* assay of STm HeLa cell invasion. mRNA transfections (with JCs) of EXPI293 resulted in functional $IgA2_{mRNA}$ that reduced STm invasion of HeLa cells to a level similar to $IgA2_R$ (Figure 1F),[25] confirming that mRNA can encode for functional oligomeric IgA proteins.

$IgA2_{mRNA}$ exhibits an increased serum half-life and N-linked sialylation of all asparagine sites as compared to $IgA2_R$

While the mucosal targeting and oligomeric properties of IgA are clinically appealing, these proteins have traditionally suffered from poor pharmacodynamic properties and, in particular, a short serum half-life.[20,29] To assess how *in vivo* production of IgA from formulated mRNA (containing HCs, LCs, and JCs) impacts pharmacodynamics, BALB/c mice were injected with 5 mg/kg $IgA2_R$ (containing a mixture of monomeric and dimeric IgA2), 4.5 mg/kg polyclonal human IgA isolated from serum (mostly monomeric), and mRNA/LNPs encoding $IgA2_{mRNA}$. Analogous to previous reports,[29] $IgA2_R$ exhibited a terminal half-life of 0.64 days and was detected for 2 days, while polyclonal human serum IgA was detected for 12 days with a terminal half-life of 0.93 days (Figure 2A). In comparison, $IgA2_{mRNA}$ exhibited a terminal half-life of 1.63 days, demonstrating a fundamental divergence from that of $IgA2_R$ (Figures 2A and 2B).

$IgA2_R$ produced in HEK293 cells has been reported to be undersialylated compared with IgA isolated from human serum,[29] resulting in rapid clearance from circulation by the asialoglycoprotein receptor (ASGPR) and other mechanisms.[20,30] To determine if we observe glycosylation differences, we quantified the levels of sialylation and overall glycosylation patterns of Sal4 $IgA2_{mRNA}$ purified from mouse serum (Figures 2C–2F and S2). As serum IgA is mostly monomeric, glycosylation patterns of $IgA2_{mRNA}$ were compared to isolated $_mIgA2_R$ or $IgA2_R$ containing monomers and dimers. $IgA2_{mRNA}$ exhibited greater N-glycosylation of the complex type (90%) compared with $IgA2_R$ (30%) and $_mIgA2_R$ (19%) (Figure S2). In contrast, high-mannose-type branched structures were predominant in $IgA2_R$ (66%) and $_mIgA2_R$ (76%), as compared with the low levels (5%) found in $IgA2_{mRNA}$. Levels of high-mannose structures correlated with a low level of sialylation (13%–14%) in $_mIgA2_R$ and $IgA2_R$, as compared with the high levels of sialylation (91% of glycan structures in all asparagine sites) of $IgA2_{mRNA}$ (Figures 2C–2F and S2). In addition, $IgA2_{mRNA}$ and $_mIgA2_R$ have minimal fucosylation (13%–14% of glycan structures at all asparagine sites; Figure S2) compared with $IgA2_R$

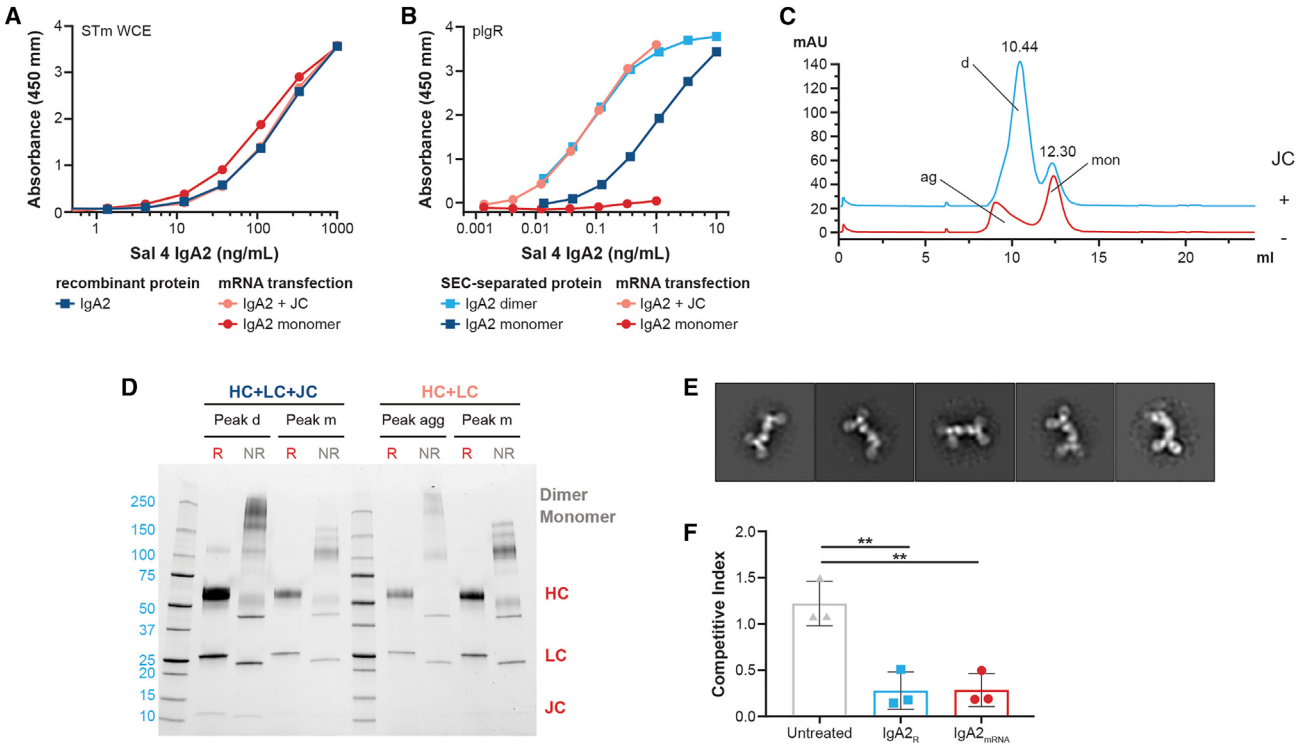

Figure 1. Characterization of Sal4 IgA2$_{mRNA}$ from *in vitro* transfection

(A) Binding of mRNA transfection supernatant and recombinant protein of Sal4 IgA2 to STm.

(B) Binding of SEC-separated Sal4 IgA2$_R$ and supernatant from mRNA-transfected Sal4 IgA2 to immobilized human pIgR.

(C) Analytical SEC of affinity-purified IgA2 from mRNA transient transfection. Dimer (d) and monomer (mon) peaks are denoted. Transfections with JC are in blue and without JC are in orange, with aggregates (ag) labeled.

(D) SDS-PAGE of designated SEC peaks from mRNA transient transfection under reducing (R) and non-reducing (NR) conditions. dimer and monomer for NR are denoted along with HCs, LCs, and JCs in R conditions.

(E) Representative image of negative-stain EM 2D class averages of the dimeric peak isolated from mRNA transfection with J chain.

(F) Effect of IgA2$_R$ or IgA2$_{mRNA}$ on STm invasion of HeLa cells. Each symbol represents a replicate, and data is graphed mean ± SD of 3 replicates, **p < 0.05.

(24%). High-mannose-type branched structures of JCs were found to predominate in IgA2$_R$, while IgA2$_{mRNA}$ and $_m$IgA2$_R$ were undetectable (Figure S2), further indicating the mostly monomeric nature of IgA2$_{mRNA}$ in circulation.

When *N*-glycosylation was examined at the individual residue level, similar trends in glycosylation patterns were observed (Figures 2C–2F). Residues N190 and N348 of IgA2$_{mRNA}$ were found to have nearly 100% complex-type glycans. In contrast, N190 and N348 of IgA2$_R$ had 31%–45% complex-type glycans. However, compared to N190 and N348, lower levels of complex-type glycans were observed on N274 and N470 in all the IgA2 preparations tested. In addition, N470 was glycosylated at low occupancy (55% for IgA2$_{mRNA}$ and 58% for $_m$IgA2$_R$) relative to the nearly complete occupancy observed at most other sites (Figures 2C–2F).

Distribution profiles of mRNA encoded IgG1 and $_d$IgA

As $_d$IgA is actively transported into mucosal secretions, we investigated whether administration of mRNA/LNP-formulated Sal4 IgA2$_{mRNA}$ results in accumulation of $_d$IgA$_{mRNA}$ in mucosal tissues. We compared Sal4 $_d$IgA2$_R$, IgA2$_{mRNA}$, and IgG serum kinetics and mucosal localization over time. Intravenous administration of IgG1$_R$ (2.5 mg/kg) to BALB/c mice resulted in the immediate appearance of Sal4 IgG in circulation (Figure 3A). At no time point was Sal4 IgG1$_R$ detectable in fecal pellets, despite the high circulating concentrations in serum (Figure 3B). Intravenous administration of an equivalent amount of $_d$IgA2$_R$ (2.5 mg/kg), on the other hand, was undetectable in the serum, potentially due to rapid transport into mucosal tissues (Figure 3A). Indeed, intravenous injection of Sal4 $_d$IgA2$_R$ resulted in detectable Sal4 IgA in fecal pellets at 6 h (Figure 3B).

In contrast to the recombinant proteins, mRNA-LNP (1 mg/kg) encoding IgG1$_{mRNA}$ and IgA2$_{mRNA}$ reached peak systemic titers of 69 and 27 μg/mL, respectively, between 24 and 48 h following injection (Figure 3A). Undetectable levels of $_d$IgA2$_R$ in circulation suggests that levels of IgA2$_{mRNA}$ in the serum at later time points are mostly monomeric, but this finding was not formally investigated. However, IgG1$_{mRNA}$ was not detectable in fecal pellets collected at 24 h, suggesting that Sal4 IgG1$_{mRNA}$ was transported into the gut at undetectable levels and/or that its half-life in intestinal secretions was extremely short (Figure 3B). In contrast, mice injected with mRNA/LNP encoding IgA2$_{mRNA}$ had Sal4 IgA in fecal pellets at 24 h (67 ng/mL) and remained detectable for 96 h (Figures 3B, 3C, S3A, and S3B).

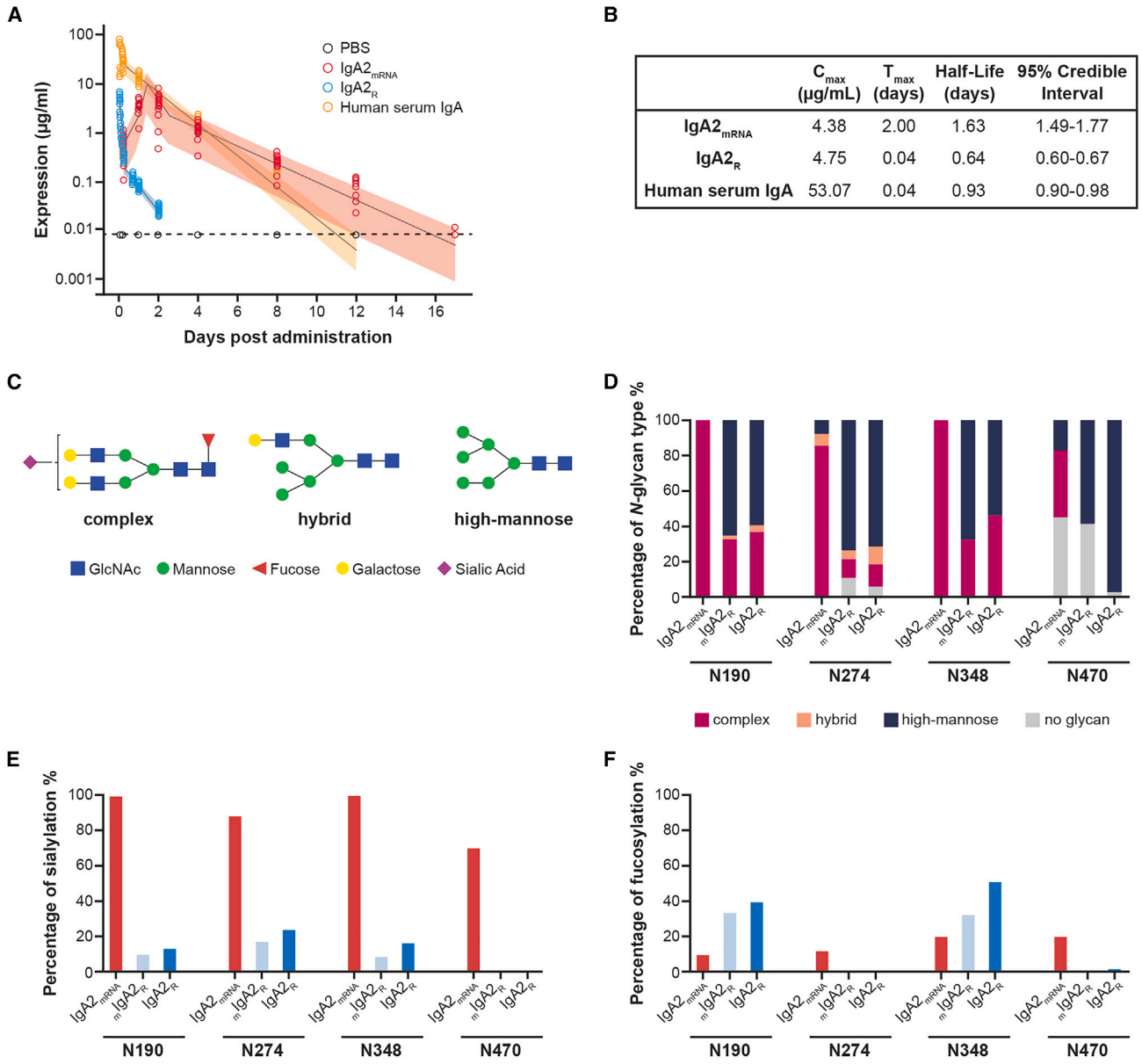

	C_{max} (µg/mL)	T_{max} (days)	Half-Life (days)	95% Credible Interval
$IgA2_{mRNA}$	4.38	2.00	1.63	1.49-1.77
$IgA2_R$	4.75	0.04	0.64	0.60-0.67
Human serum IgA	53.07	0.04	0.93	0.90-0.98

Figure 2. Characterization of $IgA2_{mRNA}$ serum half-life and site-specific glycosylation patterns *in vivo* as compared to $IgA2_R$

BALB/c mice were injected intravenously with 1 mg/kg formulated $IgA2_{mRNA}$, 5 mg/kg Sal4 $IgA2_R$, or 4.5 mg/kg IgA isolated from human serum. Concentrations of antibody were measured in serum over time by isotype-specific ELISA and modeled using a flexible linear mixed-effects model.

(A and B) Observed animal-level expression by ELISA and (A) model-based estimates of the mean and 95% credible interval and (B) model-based half-life estimates with 95% credible intervals are shown.

(C) Examples of three main types of *N*-glycan structure: complex, hybrid, and high mannose.

(D) IgA2 *N*-glycan compositions observed at 4 asparagine residues (N190, N274, N348, and N470).

(E) Sialylation of IgA2 asparagine residues, expressed as a percentage of complex and hybrid glycans that are sialylated.

(F) Fucosylation of IgA2 asparagine residues, expressed as a percentage of complex, hybrid, and high-mannose glycans that are fucosylated. Consistent detection of glycopeptides was observed across three technical executions in a serum pool from 50 animals.

$IgA2_{mRNA}$ administration results in reduced intestinal invasion by STm

We employed an established mouse model of STm intestinal invasion to determine if expression of Sal4 $IgA2_{mRNA}$ resulted in reduced infection of intestinal mucosa (Figure 3C).[25] Mice were administered 1 mg/kg mRNA/LNP encoding for Sal4 $IgA2_{mRNA}$ or IgG_{mRNA} or 5 mg/kg analogous recombinant antibody protein. Prior to challenge, serum $IgA2_{mRNA}$ levels were an average of 11 µg/mL, while $IgA2_R$ was undetectable (Figure 3D). In contrast, $IgG1_{mRNA}$ and $IgG1_R$ levels were 291 and 84 µg/mL, respectively

CellPress
OPEN ACCESS

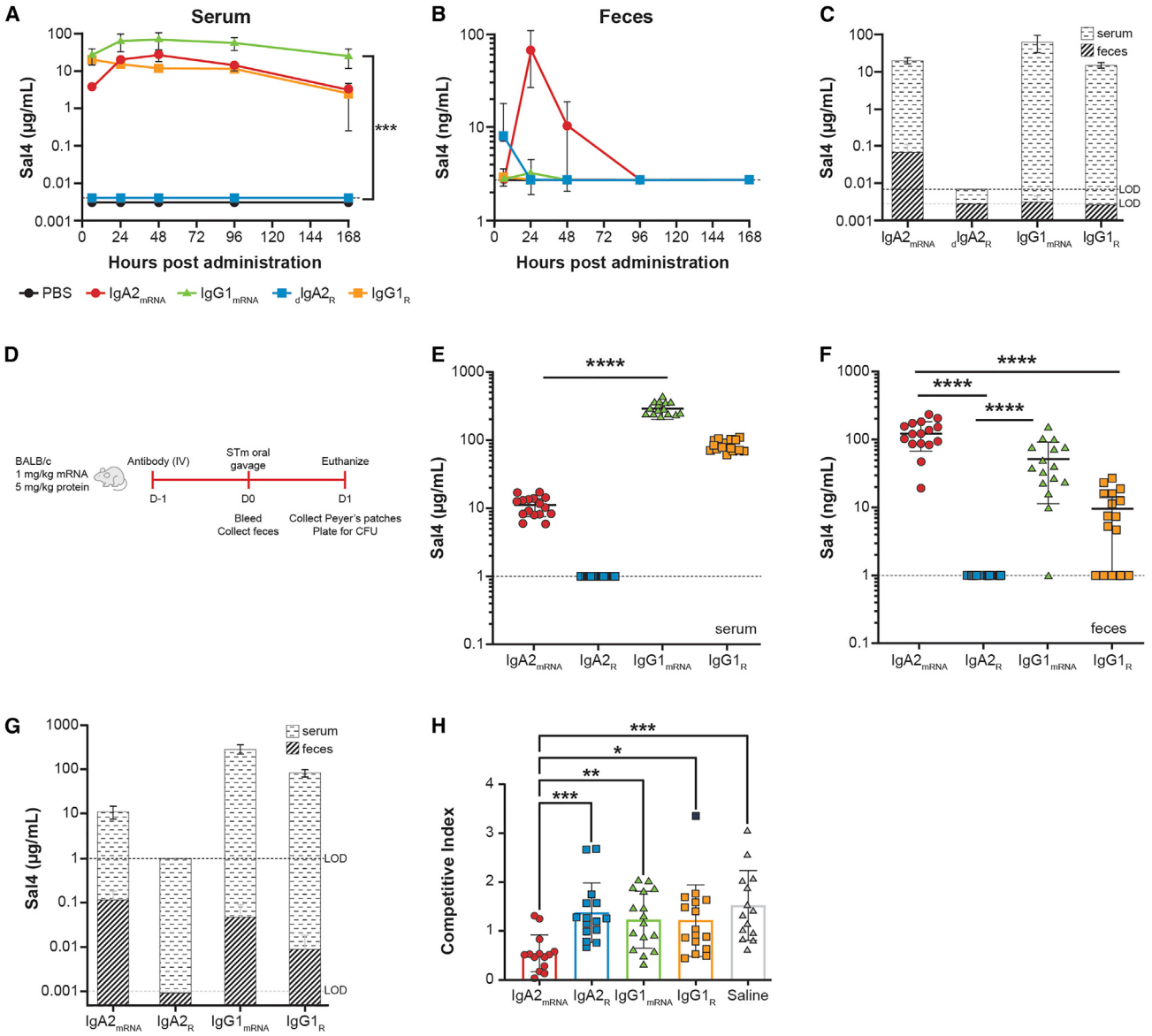

Figure 3. $IgA2_{mRNA}$ expresses in serum, traffics to mucosa, and can block STm invasion into mouse Peyer's patches

(A–C) Adult BALB/c mice were injected intravenously with 1 mg/kg formulated antibody encoded by mRNA modified with 3′idT, 2.5 mg/kg $IgG1_R$, or 2.5 mg/kg $_dIgA2_R$. Concentrations of antibody were measured in (A) serum and (B) feces over time by isotype-specific ELISA.

(C) Comparison of serum and feces levels at 24 h following administration in mice receiving different test articles.

(D) STm challenge outlined for (E)–(H) where adult BALB/c mice were injected intravenously with 1 mg/kg formulated antibody encoded by mRNA modified with 3′idT, 5 mg/kg recombinant antibody protein, or saline. Mice were challenged 24 h later with an oral gavage of a one-to-one mixture of O5+ and O5− strains (4×10^7 colony-forming units [CFUs] total).

(E and F) Concentrations of antibody were measured in (E) serum and (F) feces prior to challenge by isotype-specific ELISA.

(G) Comparison of serum and fecal antibody levels immediately prior to challenge.

(H) Competitive indices of O5+ and O5− STm. Dashed line represents the limit of detection of the assay.

Each group in (A)–(C) represents the mean ± SD of 4–8 mice per group. Each symbol in (D)–(G) represents an individual mouse with mean ± SD depicted. *$p < 0.05$, **$p < 0.01$, and ***$p < 0.001$.

(Figure 3D). However, in the fecal pellets, $IgA2_{mRNA}$ was found at the highest concentrations (average: 125 ng/mL), followed by Sal4 $IgG1_{mRNA}$ (average: 52 ng/mL) and $IgG1_R$ (average: 10 ng/mL) (Figure 3E). Detection of Sal4 IgG in the fecal pellet extracts in this experiment compared with the previous experiment may be a consequence of using mice sourced from different vendors, which can change the microbiome composition and, consequently, the intestinal barrier function.[31] The elevated levels of fecal $IgA2_{mRNA}$ relative to serum antibody levels are consistent with active transport of Sal4 $IgA2_{mRNA}$ into intestinal

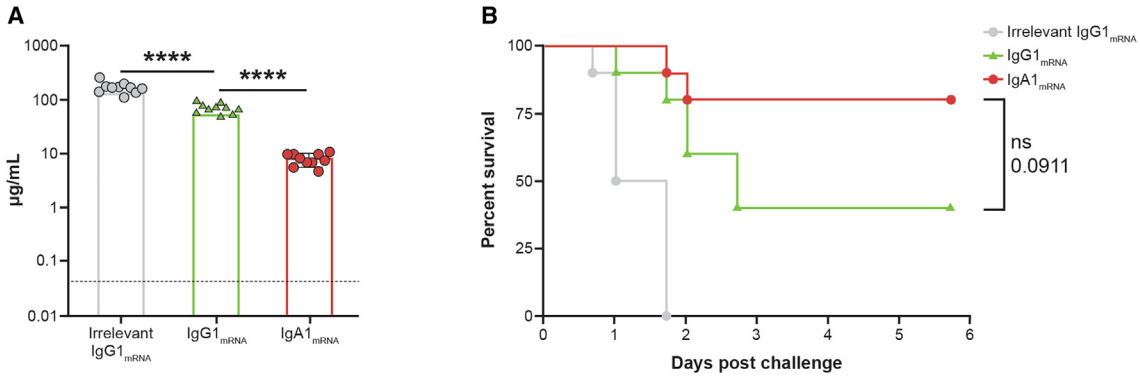

Figure 4. CAM003 IgA1$_{mRNA}$ and IgG1$_{mRNA}$ protect mice against lethal challenge in a *P. aeruginosa* acute pneumonia model

Adult BALB/c mice were injected intravenously with 1 mg/kg formulated mRNA encoding CAM003 as an IgG1 or an IgA1 and were intranasally challenged 24 h later with 6.75 $\log_{10}$ CFU *P. aeruginosa* strain PA01. Mice were monitored for survival for 6 days following challenge.

(A) Circulating antibody concentration in serum prior to challenge by isotype-specific ELISA (n = 10/group). Each symbol represents an individual mouse, and data is graphed mean ± SD, ****$p < 0.0001$

(B) Kaplan-Meier survival curves.

secretions, while the observed fecal IgG levels are consistent with transudation (Figure 3F). Importantly, IgA2$_{mRNA}$ significantly reduced invasion of intestinal tissues by STm more effectively than either IgA2$_R$ or IgG1 (Figure 3G). Protection, as defined by a competitive index (CI) of <0.5, was observed in mice with fecal Sal4 IgA2$_{mRNA}$ levels that were >100 ng/mL, suggesting a threshold of protection associated with mRNA-based delivery (Figure S3).

IgA1$_{mRNA}$ and IgG1$_{mRNA}$ protected mice against lethal challenge in a PA acute pneumonia model

We next investigated the capacity of IgA1$_{mRNA}$ to protect from PA in an acute lethal pneumonia model. CAM003, a well-characterized IgG antibody that binds Psl of PA, was class-switched to IgA1, the most common IgA isotype in the respiratory tract.[32] CAM003 IgA1$_{mRNA}$ retained its affinity for PA, bound to immobilized pIgR, and expressed at high levels in mouse serum (Figure S4). To determine baseline efficacy of this antibody, administration of both CAM003 IgG1$_R$ and IgG1$_{mRNA}$ demonstrated dose-dependent expression protection in a mouse model of PA acute pneumonia (Figure S4). Interestingly, IgG1$_{mRNA}$ administration resulted in higher levels of protection with lower systemic expression levels compared with IgG1$_R$, suggesting better localization of IgG1$_{mRNA}$ to lung tissue. This infection model was repeated to compare the efficacy between IgG and IgA. IgG1$_{mRNA}$ and IgA1$_{mRNA}$ administration resulted in systemic averages of 69 and 8 µg/mL, respectively, before intranasal challenge (Figure 4A). Despite significant differences in circulating antibody titers, both IgA1$_{mRNA}$ and IgG1$_{mRNA}$ protected mice from lethal challenge, consistent with the ability of IgA1$_{mRNA}$ to migrate to mucosal sites and demonstrating the ability of mRNA encoded IgA to protect in this pneumonia challenge model (Figure 4B).

DISCUSSION

As the predominant antibody transported into mucosal secretions, IgA serves as a first line of defense in immunity to a range of respiratory and enteric pathogens. This contrasts with IgG, which collects in secretions primarily by transudation, often following inflammation and/or physical breaks in barrier integrity.[33] The half-life of IgA, once in external fluids, also exceeds that of IgG, due to the presence of the secretory component and glycans that shield IgA from resident proteases.[34] These attributes, along with the demonstrated ability of certain IgAs to intercept and incapacitate pathogens prior to accessing mucosal tissues, have raised the prospect of deploying IgA mAbs as interventions to combat infectious diseases of the gut and upper airways. However, advances on this front have been stymied by the cost of generating uniform human $_d$IgA$_R$ mAbs at scale.

In this study, we report on the use of synthetic mRNA to encode human IgA mAbs that resemble native IgA in their biochemical, biophysical, and functional properties. Importantly, IgA$_{mRNA}$ displayed pharmacodynamics *in vivo* more like endogenous human IgA than IgA$_R$. We hypothesize that the observed dichotomy in serum half-life between IgA2$_{mRNA}$ and IgA2$_R$ could be due to differences in glycosylation patterns as a result of different cell-type expression.[20,29,35] The higher level of sialylation observed for IgA2$_{mRNA}$ is reminiscent of IgA2 isolated from human serum, and this could contribute to increased serum half-life via protection from receptor-mediated clearance. Alternatively, the high mannose glycosylation of IgA2$_R$ may contribute to faster clearance, which has been observed for IgG.[36] Lastly, observed differences in fucosylation levels between IgA2$_{mRNA}$ and IgA2$_R$ could contribute to differences in half-life[37]; however, the roles of the IgA2 core fucose in transcytosis and receptor engagement are currently unknown.[38] Importantly, glycosylation was only determined for an IgA2m1 isotype; it is currently unknown what level of sialylation is occurring on IgA1. As abnormally O-linked glycosylation on IgA1 has been associated with IgA nephropathy,[39] we are investigating both glycosylation and the pathology of repeated IgA$_{mRNA}$ dosing to fully characterize and understand the risks associated with this isotype.

Better pharmacodynamic properties *in vivo* translated to enhanced protection from mucosal bacterial challenge. mRNA/LNPs delivered intravenously resulted in accumulation of levels

of antigen-specific IgA in the gut and respiratory tract to attenuate STm and PA infections. In a stringent model of STm invasion, Sal4 $IgA2_{mRNA}$ resulted in significantly decreased bacterial burden as compared to IgA_R and IgG due to its accumulation at the site of infection. The degree of protection obtained from Sal4 $IgA2_{mRNA}$ was similar to that achieved with purified, recombinant Sal4 SIgA2 administered orally.[40] Our results are consistent with Sal4 $IgA2_{mRNA}$ intercepting STm in the intestinal lumen and blocking uptake into Peyer's patch tissues. The exact mechanism of IgA2 superiority compared with IgG in these studies is unknown; however, there are several plausible mechanisms. It has previously been demonstrated that bacteria agglutination is more efficient via Sal4 SIgA than IgG *in vitro*, potentially preventing bacterial invasion *in vivo*.[40] Alternatively, SIgA has been shown to prevent STm bacterial division, which results in "enchained growth," further accelerating pathogen clearance.[41] Lastly, the privileged access of IgA to the GI lumen cannot be discounted as a mechanism that results in superior protection from challenge compared with IgG.

We were also able to demonstrate protection from a lethal PA challenge in the lung with intravenously administered CAM003 $IgA1_{mRNA}$. Despite significant differences in circulating antibody titers, $IgA1_{mRNA}$ protected mice more efficiently from a lethal PA challenge than the analogous IgG_{mRNA}. Previously, greater protection in the lung over a native IgG was achieved by fusing a pIgR binding peptide to the Fc of CAM003 IgG1 to achieve better mucosal trafficking.[27] We hypothesize that class-switching CAM003 to IgA1 resulted in a similar phenomenon, with higher titers of antibody localized to the lung, which resulted in increased protection. Unfortunately, levels of antibody were not measured in the lung, but despite lower IgA titers in circulation, we still observed similar levels of protection from mortality between IgA and IgG groups, possibly due to IgA transport to the mucosa. While these results may not directly translate to humans, as the mucosal localization of IgA may differ significantly between humans and mice due to pIgR localization,[42,43] monoclonal IgA produced from mRNA can still serve as an important modality in the battle against infectious diseases.

Limitations of the study

While these studies represent a significant advance in technology to enable delivery of IgA mAbs, there are several limitations. All investigative studies described herein represent proof of concept for synthetic mRNA delivery of IgA mAbs. In humans, administration of an mRNA/LNP encoded for a ChikV mAb induced elevated transient cytokine responses at doses as low as 0.3 mg/kg[3]. Doses utilized in these mouse models (1 mg/kg) exceeded those tested in humans (0.1–0.6 mg/kg); additional pathology would be required to evaluate dose and safety prior to clinical use.

The mRNA/LNP platform was investigated only in the context of prophylactic delivery. This was somewhat by design, as our focus first and foremost was on establishing the platform technology using well-established mouse models in which IgA has been shown to be protective. Indeed, prophylactic IgA delivery could serve as means to interrupt outbreaks the likes of norovirus in confined situations such as on a cruise ship[44] or even to serve as a firewall in nosocomial outbreaks of *Klebsiella pneumoniae*, which currently does not have a licensed vaccine.[45] The potential of IgA delivery for mucosal infections is vast, and we are now actively focused on therapeutic applications of this technology. The data presented here and in previous studies[3,4] establish mRNA as a central platform for evaluating basic biology and therapeutics in a manner previously unattainable with protein-based approaches.

STAR★METHODS

Detailed methods are provided in the online version of this paper and include the following:

- KEY RESOURCES TABLE
- RESOURCE AVAILABILITY
  - Lead contact
  - Materials availability
  - Data and code availability
- EXPERIMENTAL MODEL AND SUBJECT DETAILS
  - Cell lines
  - Bacterial strains and growth conditions
  - Mice
- METHOD DETAILS
  - Recombinant antibody proteins
  - Generation of modified mRNA and LNPs
  - mRNA transfection for mAb expression
  - Enzyme-linked immunosorbent assay (ELISA)
  - Bacterial whole cell ELISA
  - HeLa cell invasion assay
  - Purification of Sal4 IgA
  - SDS-PAGE
  - Transmission electron microscopy (TEM) imaging
  - Expression of mAbs in mice
  - Mouse tissue processing for mAb quantification
  - Purification of IgA2 from mouse serum
  - Isolation of recombinant IgA2 monomer
  - Protein digestion
  - N-glycosylation site analysis
  - Glycopeptide enrichment
  - Mass spectrometry analysis
  - Data analysis
  - STm intragastric challenge
  - *P. aeruginosa* lethal acute pneumonia mouse model
- QUANTIFICATION AND STATISTICAL ANALYSIS
  - Statistical model for IgA half-life modeling

SUPPLEMENTAL INFORMATION

Supplemental information can be found online at https://doi.org/10.1016/j.xcrm.2023.101253.

ACKNOWLEDGMENTS

We thank Dr. Gregory Hendricks and Dr. Kyoung Hwan Lee from the Electron Microscopy Facility at UMass Chan Medical School for their support of the use of Talos L120C. At the Wadsworth Center, we thank Dr. Graham Willsey for STm strain construction, Dr. Jennifer Yates for assistance with mouse studies, and the Media and Cell Culture core facility for bacterial growth media. Medical writing and editorial assistance, under the direction of the authors, was provided by Jared Mackenzie, PhD, of MEDiSTRAVA in accordance with Good

Publication Practice (GPP3) guidelines and was funded by Moderna, Inc. The graphical abstract was made using a BioRender license. All experiments and studies were funded by Moderna.

AUTHOR CONTRIBUTIONS

Conceptualization, C.E.D., A.F.R., T.Y., D.L., R.K., N.J.M., A.C., and O.J.P.; methodology, C.E.D., A.F.R., M.J.M., Z.W., Y.-T.L., B.R.F., S.H., E.N., D.L., R.K., S.L., H.K., M.K., M.E.P., W.J.W., J.E.D., and S.K.L.; formal analysis, C.J.H., H.K., M.K., and I.L.R.; investigation, C.E.D., A.F.R., T.Y., M.J.M., Z.W., Y.-T.L., D.L., M.E.P., W.J.W., J.E.D., and S.K.L.; resources, B.R.F., S.H., E.N., S.L., M.E.P., W.J.W., N.J.M., A.C., and O.J.P.; writing – original draft, C.E.D. and D.L.; writing – review & editing, C.E.D., A.F.R., Y.-T.L., D.L., R.K., S.L., W.J.W., N.J.M., A.C., and O.J.P.; validation, A.F.R., T.Y., J.E.D., and S.K.L.; supervision, Y.-T.L., R.K., S.L., N.J.M., A.C., and O.J.P.; project administration, N.J.M., W.J.W., A.C., and O.J.P.

DECLARATION OF INTERESTS

C.E.D., A.F.R., T.Y., M.J.M., Z.W., Y.-T.L., B.R.F., S.H., D.L., R.K., S.L., C.J.H., I.L.R., H.K., M.K., A.C., and O.J.P. are employees of and shareholders in Moderna, Inc. C.E.D. and O.J.P. are co-inventors on international patent WO 2022/212191 A1. E.N. was an employee of and shareholder in Moderna Inc. at the time of the study.

INCLUSION AND DIVERSITY

We support inclusive, diverse, and equitable conduct of research.

Received: April 6, 2023
Revised: July 28, 2023
Accepted: September 29, 2023
Published: November 1, 2023

REFERENCES

1. Kyriakidis, N.C., López-Cortés, A., González, E.V., Grimaldos, A.B., and Prado, E.O. (2021). SARS-CoV-2 vaccines strategies: a comprehensive review of phase 3 candidates. NPJ Vaccines *6*, 28. https://doi.org/10.1038/s41541-021-00292-w.
2. Chaudhary, N., Weissman, D., and Whitehead, K.A. (2021). mRNA vaccines for infectious diseases: principles, delivery and clinical translation. Nat. Rev. Drug Discov. *20*, 817–838. https://doi.org/10.1038/s41573-021-00283-5.
3. August, A., Attarwala, H.Z., Himansu, S., Kalidindi, S., Lu, S., Pajon, R., Han, S., Lecerf, J.M., Tomassini, J.E., Hard, M., et al. (2021). A phase 1 trial of lipid-encapsulated mRNA encoding a monoclonal antibody with neutralizing activity against Chikungunya virus. Nat. Med. *27*, 2224–2233. https://doi.org/10.1038/s41591-021-01573-6.
4. Narayanan, E., Falcone, S., Elbashir, S.M., Attarwala, H., Hassett, K., Seaman, M.S., Carfi, A., and Himansu, S. (2022). Rational design and in vivo characterization of mRNA-encoded broadly neutralizing antibody combinations against HIV-1. Antibodies *11*, 67.
5. Steffen, U., Koeleman, C.A., Sokolova, M.V., Bang, H., Kleyer, A., Rech, J., Unterweger, H., Schicht, M., Garreis, F., Hahn, J., et al. (2020). IgA subclasses have different effector functions associated with distinct glycosylation profiles. Nat. Commun. *11*, 120. https://doi.org/10.1038/s41467-019-13992-8.
6. Li, Y., Jin, L., and Chen, T. (2020). The effects of secretory IgA in the mucosal immune system. BioMed Res. Int. *2020*, 2032057. https://doi.org/10.1155/2020/2032057.
7. Bertrand, Y., Sánchez-Montalvo, A., Hox, V., Froidure, A., and Pilette, C. (2023). IgA-producing B cells in lung homeostasis and disease. Front. Immunol. *14*, 1117749. https://doi.org/10.3389/fimmu.2023.1117749.
8. Brandtzaeg, P., and Prydz, H. (1984). Direct evidence for an integrated function of J chain and secretory component in epithelial transport of immunoglobulins. Nature *311*, 71–73. https://doi.org/10.1038/311071a0.
9. Macpherson, A.J., Geuking, M.B., and McCoy, K.D. (2012). Homeland security: IgA immunity at the frontiers of the body. Trends Immunol. *33*, 160–167. https://doi.org/10.1016/j.it.2012.02.002.
10. Matsumoto, M.L. (2022). Molecular mechanisms of multimeric assembly of IgM and IgA. Annu. Rev. Immunol. *40*, 221–247. https://doi.org/10.1146/annurev-immunol-101320-123742.
11. Hausmann, A., Böck, D., Geiser, P., Berthold, D.L., Fattinger, S.A., Furter, M., Bouman, J.A., Barthel-Scherrer, M., Lang, C.M., Bakkeren, E., et al. (2020). Intestinal epithelial NAIP/NLRC4 restricts systemic dissemination of the adapted pathogen Salmonella Typhimurium due to site-specific bacterial PAMP expression. Mucosal Immunol. *13*, 530–544. https://doi.org/10.1038/s41385-019-0247-0.
12. Bakkeren, E., Huisman, J.S., Fattinger, S.A., Hausmann, A., Furter, M., Egli, A., Slack, E., Sellin, M.E., Bonhoeffer, S., Regoes, R.R., et al. (2019). Salmonella persisters promote the spread of antibiotic resistance plasmids in the gut. Nature *573*, 276–280. https://doi.org/10.1038/s41586-019-1521-8.
13. Jennings, L.K., Dreifus, J.E., Reichhardt, C., Storek, K.M., Secor, P.R., Wozniak, D.J., Hisert, K.B., and Parsek, M.R. (2021). Pseudomonas aeruginosa aggregates in cystic fibrosis sputum produce exopolysaccharides that likely impede current therapies. Cell Rep. *34*, 108782. https://doi.org/10.1016/j.celrep.2021.108782.
14. Richards, A., Baranova, D., and Mantis, N.J. (2022). The prospect of orally administered monoclonal secretory IgA (SIgA) antibodies to prevent enteric bacterial infections. Hum. Vaccines Immunother. *18*, 1964317. https://doi.org/10.1080/21645515.2021.1964317.
15. Yamane-Ohnuki, N., and Satoh, M. (2009). Production of therapeutic antibodies with controlled fucosylation. mAbs *1*, 230–236. https://doi.org/10.4161/mabs.1.3.8328.
16. Solá, R.J., and Griebenow, K. (2009). Effects of glycosylation on the stability of protein pharmaceuticals. J. Pharmaceut. Sci. *98*, 1223–1245. https://doi.org/10.1002/jps.21504.
17. Flintegaard, T.V., Thygesen, P., Rahbek-Nielsen, H., Levery, S.B., Kristensen, C., Clausen, H., and Bolt, G. (2010). N-glycosylation increases the circulatory half-life of human growth hormone. Endocrinology *151*, 5326–5336. https://doi.org/10.1210/en.2010-0574.
18. Li, C.W., Lim, S.O., Xia, W., Lee, H.H., Chan, L.C., Kuo, C.W., Khoo, K.H., Chang, S.S., Cha, J.H., Kim, T., et al. (2016). Glycosylation and stabilization of programmed death ligand-1 suppresses T-cell activity. Nat. Commun. *7*, 12632. https://doi.org/10.1038/ncomms12632.
19. Meyer, S., Nederend, M., Jansen, J.H.M., Reiding, K.R., Jacobino, S.R., Meeldijk, J., Bovenschen, N., Wuhrer, M., Valerius, T., Ubink, R., et al. (2016). Improved in vivo anti-tumor effects of IgA-Her2 antibodies through half-life extension and serum exposure enhancement by FcRn targeting. mAbs *8*, 87–98. https://doi.org/10.1080/19420862.2015.1106658.
20. Rouwendal, G.J., van der Lee, M.M., Meyer, S., Reiding, K.R., Schouten, J., de Roo, G., Egging, D.F., Leusen, J.H., Boross, P., Wuhrer, M., et al. (2016). A comparison of anti-HER2 IgA and IgG1 in vivo efficacy is facilitated by high N-glycan sialylation of the IgA. mAbs *8*, 74–86. https://doi.org/10.1080/19420862.2015.1102812.
21. Xiao, Y., Zhang, Y., Wang, Z., Zhao, W., Xu, X., Chen, X., Tan, F., Sun, Z., Huang, B., and Tian, K. (2022). A therapeutic chimeric IgG/IgA expressed by CHO cells for oral treatment of PED in piglets. Front. Microbiol. *13*, 1018748. https://doi.org/10.3389/fmicb.2022.1018748.
22. Albaugh, G.P., Dutta, S.K., Iyengar, V., Shami, S., Lohani, A., Sainz, E., Kessie, G., Nair, P., Lagerholm, S., Kamra, A., et al. (2020). Identification of a native novel oncolytic immunoglobulin on exfoliated colon epithelial

cells: A bispecific heterodimeric chimera of IgA/IgG Open. Open J. Prev. Med. *10*, 126–150.

23. Li, C., An, X., Butt, A.M., Zhang, B., Zhang, Z., Wang, X., Huang, Y., Zhang, W., Zhang, B., Mi, Z., and Tong, Y. (2014). Construction of a chimeric secretory IgA and its neutralization activity against avian influenza virus H5N1. J. Immunol. Res. *2014*, 394127. https://doi.org/10.1155/2014/394127.

24. Michetti, P., Mahan, M.J., Slauch, J.M., Mekalanos, J.J., and Neutra, M.R. (1992). Monoclonal secretory immunoglobulin A protects mice against oral challenge with the invasive pathogen Salmonella typhimurium. Infect. Immun. *60*, 1786–1792. https://doi.org/10.1128/iai.60.5.1786-1792.1992.

25. Richards, A.F., Doering, J.E., Lozito, S.A., Varrone, J.J., Willsey, G.G., Pauly, M., Whaley, K., Zeitlin, L., and Mantis, N.J. (2020). Inhibition of invasive salmonella by orally administered IgA and IgG monoclonal antibodies. PLoS Neglected Trop. Dis. *14*, e0007803. https://doi.org/10.1371/journal.pntd.0007803.

26. DiGiandomenico, A., Warrener, P., Hamilton, M., Guillard, S., Ravn, P., Minter, R., Camara, M.M., Venkatraman, V., Macgill, R.S., Lin, J., et al. (2012). Identification of broadly protective human antibodies to Pseudomonas aeruginosa exopolysaccharide Psl by phenotypic screening. J. Exp. Med. *209*, 1273–1287. https://doi.org/10.1084/jem.20120033.

27. Borrok, M.J., DiGiandomenico, A., Beyaz, N., Marchetti, G.M., Barnes, A.S., Lekstrom, K.J., Phipps, S.S., McCarthy, M.P., Wu, H., Dall'Acqua, W.F., et al. (2018). Enhancing IgG distribution to lung mucosal tissue improves protective effect of anti-Pseudomonas aeruginosa antibodies. JCI Insight *3*, e97844. https://doi.org/10.1172/jci.insight.97844.

28. Xie, Y., He, L., Lugano, R., Zhang, Y., Cao, H., He, Q., Chao, M., Liu, B., Cao, Q., Wang, J., et al. (2021). Key molecular alterations in endothelial cells in human glioblastoma uncovered through single-cell RNA sequencing. JCI Insight *6*, e150861. https://doi.org/10.1172/jci.insight.150861.

29. Lombana, T.N., Rajan, S., Zorn, J.A., Mandikian, D., Chen, E.C., Estevez, A., Yip, V., Bravo, D.D., Phung, W., Farahi, F., et al. (2019). Production, characterization, and in vivo half-life extension of polymeric IgA molecules in mice. mAbs *11*, 1122–1138. https://doi.org/10.1080/19420862.2019.1622940.

30. Rifai, A., Fadden, K., Morrison, S.L., and Chintalacharuvu, K.R. (2000). The N-glycans determine the differential blood clearance and hepatic uptake of human immunoglobulin (Ig)A1 and IgA2 isotypes. J. Exp. Med. *191*, 2171–2182. https://doi.org/10.1084/jem.191.12.2171.

31. Ivanov, I.I., Atarashi, K., Manel, N., Brodie, E.L., Shima, T., Karaoz, U., Wei, D., Goldfarb, K.C., Santee, C.A., Lynch, S.V., et al. (2009). Induction of intestinal Th17 cells by segmented filamentous bacteria. Cell *139*, 485–498. https://doi.org/10.1016/j.cell.2009.09.033.

32. Janeway C, A., Travers, P., and M, W. (2001). Immunobiology: The Immune System in Health and Disease, 5th edition Edition (Garland Science).

33. Castro-Dopico, T., and Clatworthy, M.R. (2019). IgG and Fcgamma receptors in intestinal immunity and inflammation. Front. Immunol. *10*, 805. https://doi.org/10.3389/fimmu.2019.00805.

34. Chintalacharuvu, K.R., Chuang, P.D., Dragoman, A., Fernandez, C.Z., Qiu, J., Plaut, A.G., Trinh, K.R., Gala, F.A., and Morrison, S.L. (2003). Cleavage of the human immunoglobulin A1 (IgA1) hinge region by IgA1 proteases requires structures in the Fc region of IgA. Infect. Immun. *71*, 2563–2570.

35. Sabnis, S., Kumarasinghe, E.S., Salerno, T., Mihai, C., Ketova, T., Senn, J.J., Lynn, A., Bulychev, A., McFadyen, I., Chan, J., et al. (2018). A novel amino lipid series for mRNA delivery: improved endosomal escape and sustained pharmacology and safety in non-human primates. Mol. Ther. *26*, 1509–1519. https://doi.org/10.1016/j.ymthe.2018.03.010.

36. Goetze, A.M., Liu, Y.D., Zhang, Z., Shah, B., Lee, E., Bondarenko, P.V., and Flynn, G.C. (2011). High-mannose glycans on the Fc region of therapeutic IgG antibodies increase serum clearance in humans. Glycobiology *21*, 949–959. https://doi.org/10.1093/glycob/cwr027.

37. Ferrara, C., Grau, S., Jäger, C., Sondermann, P., Brünker, P., Waldhauer, I., Hennig, M., Ruf, A., Rufer, A.C., Stihle, M., et al. (2011). Unique carbohydrate-carbohydrate interactions are required for high affinity binding between FcgammaRIII and antibodies lacking core fucose. Proc. Natl. Acad. Sci. USA *108*, 12669–12674. https://doi.org/10.1073/pnas.1108455108.

38. Schneider, M., Al-Shareffi, E., and Haltiwanger, R.S. (2017). Biological functions of fucose in mammals. Glycobiology *27*, 601–618. https://doi.org/10.1093/glycob/cwx034.

39. Suzuki, H., Moldoveanu, Z., Hall, S., Brown, R., Vu, H.L., Novak, L., Julian, B.A., Tomana, M., Wyatt, R.J., Edberg, J.C., et al. (2008). IgA1-secreting cell lines from patients with IgA nephropathy produce aberrantly glycosylated IgA1. J. Clin. Invest. *118*, 629–639. https://doi.org/10.1172/JCI33189.

40. Richards, A.F., Baranova, D.E., Pizzuto, M.S., Jaconi, S., Willsey, G.G., Torres-Velez, F.J., Doering, J.E., Benigni, F., Corti, D., and Mantis, N.J. (2021). Recombinant human secretory IgA induces salmonella typhimurium agglutination and limits bacterial Invasion into gut-associated lymphoid tissues. ACS Infect. Dis. *7*, 1221–1235. https://doi.org/10.1021/acsinfecdis.0c00842.

41. Moor, K., Diard, M., Sellin, M.E., Felmy, B., Wotzka, S.Y., Toska, A., Bakkeren, E., Arnoldini, M., Bansept, F., Co, A.D., et al. (2017). High-avidity IgA protects the intestine by enchaining growing bacteria. Nature *544*, 498–502. https://doi.org/10.1038/nature22058.

42. P Vaerman, J., Lemaître-Coelho, I.M., Limet, J.N., et al. (1982). In Hepatic transfer of polymeric IgA from plasma to bile in rats and other mammals: a survey, W. Strober, L.A. Hanson, and K. Sell, eds. (Raven Press).

43. Snoeck, V., Peters, I.R., and Cox, E. (2006). The IgA system: a comparison of structure and function in different species. Vet. Res. *37*, 455–467. https://doi.org/10.1051/vetres:2006010.

44. Alvarado, G., Ettayebi, K., Atmar, R.L., Bombardi, R.G., Kose, N., Estes, M.K., and Crowe, J.E., Jr. (2018). Human Monoclonal Antibodies That Neutralize Pandemic GII.4 Noroviruses. Gastroenterology *155*, 1898–1907. https://doi.org/10.1053/j.gastro.2018.08.039.

45. Cohen, T.S., Pelletier, M., Cheng, L., Pennini, M.E., Bonnell, J., Cvitkovic, R., Chang, C.S., Xiao, X., Cameroni, E., Corti, D., et al. (2017). Anti-LPS antibodies protect against Klebsiella pneumoniae by empowering neutrophil-mediated clearance without neutralizing TLR4. JCI Insight *2*, e92774. https://doi.org/10.1172/jci.insight.92774.

46. Forbes, S.J., Eschmann, M., and Mantis, N.J. (2008). Inhibition of Salmonella enterica serovar typhimurium motility and entry into epithelial cells by a protective antilipopolysaccharide monoclonal immunoglobulin A antibody. Infect. Immun. *76*, 4137–4144. https://doi.org/10.1128/iai.00416-08.

47. Forbes, S.J., Martinelli, D., Hsieh, C., Ault, J.G., Marko, M., Mannella, C.A., and Mantis, N.J. (2012). Association of a protective monoclonal IgA with the O antigen of Salmonella enterica serovar Typhimurium impacts type 3 secretion and outer membrane integrity. Infect. Immun. *80*, 2454–2463. https://doi.org/10.1128/iai.00018-12.

48. Nelson, J., Sorensen, E.W., Mintri, S., Rabideau, A.E., Zheng, W., Besin, G., Khatwani, N., Su, S.V., Miracco, E.J., Issa, W.J., et al. (2020). Impact of mRNA chemistry and manufacturing process on innate immune activation. Sci. Adv. *6*, eaaz6893. https://doi.org/10.1126/sciadv.aaz6893.

49. Cao, L., Diedrich, J.K., Ma, Y., Wang, N., Pauthner, M., Park, S.K.R., Delahunty, C.M., McLellan, J.S., Burton, D.R., Yates, J.R., and Paulson, J.C. (2018). Global site-specific analysis of glycoprotein N-glycan processing. Nat. Protoc. *13*, 1196–1212. https://doi.org/10.1038/nprot.2018.024.

50. Liu, D., Wang, S., Zhang, J., Xiao, W., Miao, C.H., Konkle, B.A., Wan, X.F., and Li, L. (2021). Site-specific N- and O-glycosylation analysis of human

plasma fibronectin. Front. Chem. *9*, 691217. https://doi.org/10.3389/fchem.2021.691217.

51. Watanabe, Y., Allen, J.D., Wrapp, D., McLellan, J.S., and Crispin, M. (2020). Site-specific glycan analysis of the SARS-CoV-2 spike. Science *369*, 330–333. https://doi.org/10.1126/science.abb9983.
52. Varki, J., Cummings, R.D., Esko, J.D., Stanley, P., Hart, G.W., Aebi, M., Mohnen, D., Kinoshita, T., Packer, N.H., Prestegard, J.H., et al. (2015). Essentials of Glycobiology (Cold Spring Harbor (NY): Laboratory Press).
53. Wood, S.N. (2003). Thin plate regression splines. J. Roy. Stat. Soc. B *65*, 95–114. https://doi.org/10.1111/1467-9868.00374.
54. Bürkner, P.-C. (2017). brms: An R Package for Bayesian Multilevel Models Using Stan. J. Stat. Software *80*, 1–28. https://doi.org/10.18637/jss.v080.i01.

STAR★METHODS

KEY RESOURCES TABLE

REAGENT or RESOURCE	SOURCE	IDENTIFIER
Antibodies		
CAM003 IgG	GeneArt	N/A
Sal4 IgG	Genscript	N/A
Sal4 IgA2m1	GeneArt	N/A
CAM003 IgA1	GeneArt	N/A
Goat anti human IgG Fc fragment	Bethyl	A80-104A; RRID:AB_67060
Goat anti human IgA	Bethyl	A80-102A; RRID:AB_67044
Goat anti human IgG HRP	Southern Biotech	2040–05; RRID:AB_2795644
Goat anti human lambda HRP	Bethyl	A80-116P; RRID:AB_67591
Goat anti human IgA HRP	Southern Biotech	2050–05; RRID:AB_2687526
Bacterial and virus strains		
Salmonella enterica serovar Typhimurium (STm)	ATCC	14028s
S. Typhimurium strain GGW445 (*sj8101::kan oafA126::*TN*10d*-Tc *fkpA-lacZ)*	This study	GGW445
S. Typhimurium strain GGW444 (*zj8101::kan*)	This study	GGW444
Pseudomonas aeruginosa PA01	ATCC	15692
Biological samples		
Normal goat serum	Gibco	16210072
Fetal bovine serum	Gibco	16140089
Mouse serum, feces, and intestines	This study	N/A
Chemicals, peptides, and recombinant proteins		
Opti-MEM I	Gibco	31895–070
Dulbeco's Modified Media (DMEM)	Gibco	11965–092
Expi 293 expression medium	Gibco	A14351-01
CaptureSelect™ IgA affinity matrix	ThermoFisher	194288010
MabSelect SuRe™	Cytiva	17547402
carbonate-bicarbonate buffer capsules	Sigma	C3041-100CAP
Recombinant human pIgR	R&D Biosystems	2717-PG-05
10x PBS-T (0.5% Tween 20 pH 7.4)	Boston Bioproducts Inc	IBB-171
Superblock PBST	ThermoFisher	37515
Sureblue TMB 1-C substrate	SeraCare	5120–0074
TMB Stop solution	SeraCare	5150–0021
1X Phosphate buffered saline (PBS)	Cytiva	SH30256.02
Hanks' Balanced Salt Solution (HBSS)	Sigma-Aldrich	H9269-500ML
Kanamycin	Sigma-Aldrich	K4000
X-gal	RPI	B71800
Gentamicin	Sigma-Aldrich	G1264
Triton X-100	Sigma-Aldrich	T8787
Hydrochloric Acid	Fisher Scientific	A144S-212
glycine	Sigma-Aldrich	50046-50G
1M Tris-HCl, pH8.0	ThermoFisher	15568025
4x Laemmli Sample buffer	Bio-Rad	1610747
Precision Plus Protein™ standard, strep-tagged recombinant	Bio-Rad	1610363
Novex™ Tris-Glycine SDS Running Buffer (10X)	ThermoFisher	LC2675
2-mercaptoethanol (>99%)	Millipore Sigma	M6250-100ML

(*Continued on next page*)

Continued

REAGENT or RESOURCE	SOURCE	IDENTIFIER
Protease inhibitor mini tablets	ThermoFisher	A32953
Peptide M agarose	Invivogen	Gel-pdm-5
Urea	Sigma-Aldrich	U5378-500G
Tris-HCl buffer, pH 7.8	Invitrogen	15567–027
Dithiothreitol	Sigma-Aldrich	D9779-5G
Iodoacetamide	Sigma-Aldrich	I1149-5G
Glu-Glu	Sigma-Aldrich	G3640
Endoproteinase GluC	New England Biolabs	P8100S
Trypsin	Promega	V5111
	Gibco	25300–054
Formic acid	Fisher Scientific	A11710X1-AMP
Ammonium bicarbonate	Sigma-Aldrich	A6141-25G
PNGase F	Sigma-Aldrich	F8435-50UN
ZIC-HILIC particles	Nest Group Inc	200-001-0050
LC-MS grade water	Fisher Scientific	W64
LC-MS grade acetonitrile	Fisher Scientific	A955-4
LC-MS grade water with 0.1% Trifluoroacetic Acid	Fisher Scientific	LS119-1
LC-MS grade acetonitrile with 0.1% Trifluoroacetic Acid	Fisher Scientific	LS121-1
Critical commercial assays		
trans IT mRNA transfection kit	Mirus Bio LLC	MIR 2256
Amicon Ultra-15 Centrifugal Filter 50kDa MWCO	Millipore	UFC905024
Amicon Ultra-15 Centrifugal Filter 100kDa MWCO	Millipore	UFC910024
96 well NUNC Maxisorp plates	ThermoScientific	12565135S23
ImmunIon 4HBX plates	Thermo Fisher Scientific	3855
4-20% Mini-PROTEAN® TGX Stain-Free™ protein gels, 10 well, 30uL	Bio-Rad	4568093
Carbon-coated copper grid	Electron Microscopy	CF300-Cu
HiTrap Protein An HP	Cytiva	17040301
Superdex 200 Increase 10/300 GL gel filtration column	Cytiva	28990944
2.8mm ceramic beads	Thermo Fisher	15-340-154
100kDa Pierce Protein Concentrators PES	Thermo Fisher	88533
Hypersep C18 Cartridges	Thermo Scientific	03-251-259
C4 HyperSep tips	Thermo Fisher	60109–211
Easy-Spray PepMap *Neo* C18 75umx500mm column	Thermo Fisher	ES75500PN
20mm nanoEase C18 Trap Column	Water Corporation	186008821
Experimental models: Cell lines		
EXPI293F	ThermoFisher	A14527
HeLa	ATCC	CCL-2
Experimental models: Organisms/strains		
Balb/c mice (female)	Charles River Laboratories	BALB/cAnNCrl
Balb/c mice (female)	Taconic Biosciences	BALB-F
Balb/c mice (female)	Envigo Laboratories	BALB/cAnNHsd
Software and algorithms		
GraphPad Prism 9	GraphPad	9.3.1
Relion 4.0		N/A
R package brms (version 2.17.3)		N/A
Proteome Discoverer	Thermo Fisher	2.5.0.400
Byonic	Protein Metrics Inc	V3.2.0

CellPress
OPEN ACCESS

RESOURCE AVAILABILITY

Lead contact

Further information and requests for resources and reagents can be directed to the lead contact, Cailin Deal (cailin.deal@modernatx.com)

Materials availability

All reagents are commercially available and this study did not result in any new reagents.

Data and code availability

All data supporting the findings of this study are found within the paper and its supplemental information. They are also available from the lead contact upon request.

EXPERIMENTAL MODEL AND SUBJECT DETAILS

Cell lines

Expi293F cells were obtained from ThermoFisher (A14527) and maintained in Expi293 expression medium (ThermoFisher) in an Infors incubator with 5% CO_2 shaking at 120 rpm. HeLa cells were obtained from ATCC (Cat. # CCL-2) and maintained in Dulbecco's Modified Media (DMEM) with 10% fetal bovine serum at 37°C and 5% CO_2.

Bacterial strains and growth conditions

Salmonella enterica serovar Typhimurium (STm) was purchased from ATCC (ATCC 14028s). *S. Typhimurium* strains GGW445 (*sj8101::kan oafA126::*TN*10d*-Tc *fkpA-lacZ*) and GGW444 (*zj8101::kan*) with the O4 and O5 O-Ag, respectively, are derivatives of ATCC 14028s[25,46,47] *Pseudomonas aeruginosa* PA01 strain was purchased from ATCC (ATCC 15692).

Mice

Female BALB/c mice, 6 to 10 week old, were obtained from Charles River Laboratory and maintained at Moderna in Cambridge, MA. All mouse studies were approved by the Animal Care and Use Committee at Moderna. For studies performed at the Wadsworth Center, female Balb/c mice, aged 8–12 weeks, were obtained from Taconic Biosciences and were cared for by the Wadsworth Center Animal Core Facility. All experiments were performed in accordance with protocols approved by the Wadsworth Center's IACUC. Finally, all mouse studies performed at the University of North Texas Health Science Center at Fort Worth were approved by their Animal Care and Use Committee and conducted according to IACUC protocol 2019-0030. These studies utilized female Balb/c mice, aged 6–8 weeks old, that were obtained from Envigo Laboratories.

METHOD DETAILS

Recombinant antibody proteins

Recombinant protein versions of all monoclonal antibodies were purchased from Genscript or GeneArt (ThermoFisher). CAM003 IgG (GeneArt) was purified from transient transfection of a 2:1 ratio of HC to LC by weight in EXPI293 with HiTrap Protein An HP and polished using HiLoad Superdex 200 26/600 prep. Sal4 IgG (Genscript) was purified from transient transfection of HD CHO-S cells with MabSelect SuRe LX. Sal4 IgA2m1 (GeneArt) was purified from transient transfection of a 4:4:1 ratio of HC to LC to JC (by weight) in EXPI293 with CaptureSelect IgA Affinity matrix. All protein concentrations were determined by absorption at 280nm using NanoDrop.

Generation of modified mRNA and LNPs

Sequence-optimized mRNA encoding functional IgA monoclonal antibodies were synthesized *in vitro* using an optimized T7 RNA polymerase-mediated transcription reaction with complete replacement of uridine by N1-methyl-pseudouridine.[48] The reactions included a DNA template containing an open reading frame flanked by 5′ untranslated region (UTR) and 3′ UTR sequences with a terminal encoded polyA tail. Where indicated, inverted deoxythymidine (idT) were appended to the 3′ terminus of fully synthesized mRNA by phosphodiester linkage of a modifying oligo with 3′ idT. Free and end-stabilized mRNA were purified, buffer exchanged and sterile filtered.

Lipid nanoparticle-formulated mRNA was produced through a modified ethanol-drop nanoprecipitation process as described previously.[35] Briefly, ionizable, structural, helper, and polyethylene glycol lipids were mixed with mRNA (2:1 HC to LC for IgG; 4:4:1 HC to LC to JC for IgA) in acetate buffer at a pH of 5.0 and at a ratio of 3:1 (lipids:mRNA). The mixture was neutralized with Tris-Cl at a pH 7.5, sucrose was added as a cryoprotectant, and the final solution was sterile filtered. Vials were filled with formulated LNP and stored frozen at −70°C until further use. The drug product underwent analytical characterization, which included the determination of particle size and polydispersity, encapsulation, mRNA purity, osmolality, pH, endotoxin and bioburden, and the material was deemed acceptable for *in vivo* study.

mRNA transfection for mAb expression

EXPI293 cells were transiently transfected with the corresponding mRNA encoding for Sal4 IgG, Sal4 IgA2m1, CAM003 IgG or CAM003 IgA1 HC, LC and/or JC using *trans* IT-mRNA Transfection Kit (Mirus Bio LLC) per the manufacturer's recommendations. For all IgG isotypes, this required co-transfection of HC and LC at a 2:1 ratio by weight, whereas all IgA isotypes consisted of HC, LC, and JC transfections at a 4:4:1 ratio by weight, unless otherwise stated that JC was not included. EXPI293 cells were diluted to $1x10^6$ cells/mL with EXPI293 Expression Medium (ThermoFisher). Using a ratio of 1 μg mRNA per 1 mL of culture, mRNA was first added to Opti-MEM I SFM (Gibco), followed by addition of TransIT-mRNA transfection reagent (Mirus Bio) at a 1:2 ratio of mRNA to TransIT. The complex was allowed to form for 3 min before addition to the suspension culture. For DNA transfections, EXPI293 cells were transfected at $3x10^6$ cells/mL using 1 μg plasmid DNA per mL of culture. DNA complexes were formed by separately diluting DNA and Turbo293 Transfection reagent (Speed Biosystems) in Opti-MEM I, then combined and allowed to incubate at RT for 20 min before adding to suspension culture. At 48 h following transfection, cell cultures were centrifuged, and supernatant was collected. Unless being purified, majority of supernatant was further concentrated in 50–100 kdA Amicon filters for 40 min at 3000 x g. Transfection supernatants and concentrated supernatants were further used to quantitate and characterize by enzyme-linked immunosorbent assay (ELISA).

Enzyme-linked immunosorbent assay (ELISA)

To quantitate total human IgG (hIgG) or IgA (hIgA), 96-well NUNC Maxisorp plates (ThermoScientific) or Immulon 4HBX plates (Thermo Fisher Scientific) were coated with 0.1 mL per well of goat anti-human IgG Fc fragment (Bethyl A80-104A) or goat anti-human IgA (Bethyl A80-102A) at 1:100 dilution in 0.05 M carbonate-bicarbonate (Sigma C30411) overnight at 4°C. To determine binding to human pIgR, Nunc maxisorp plates were coated with 2 μg/mL of recombinant human pIgR (R&D Biosystems 2717-PG-05) at 4°C overnight. For both isotype-specific and pIgR ELISA, plates were washed with an automated plate washer (Biotek) or 4x with 0.05% PBS-T and were subsequently blocked with 0.2 mL per well of Superblock PBST (ThermoFisher) or 2% goat serum in PBS-T for 2 h at room temperature. Using purified antibodies as a standard, mRNA transfection supernatant or mouse serum was serially diluted in PBST in a dilution plate and 0.1mL per well was transferred to the coated plates and incubated for 1 to 2 h at room temperature. Following incubation, plates were subsequently washed and incubated with 0.1 mL per well of goat anti-human IgG horseradish peroxidase (HRP; Southern Biotech; 1:5000), goat anti-human lambda HRP (Bethyl; 1:10000), goat anti-human kappa HRP (Bethyl; 1:10000) or goat anti-human IgA HRP (Southern Biotech; 1:5000) for 1 h at room temperature. Plates were subsequently washed and incubated with 0.1 mL per well of Sureblue TMB 1-C substrate (Fisher Scientific) for 5 min. The reaction was stopped with 0.1 mL per well of TMB Stop solution (SeraCare) and read at an absorbance of 450nm on a SpectraMax ABS Microplate Reader or a SpectraMax iD3 Microplate Reader (Molecular Devices). Absolute quantities of human antibody in transfection supernatant or mouse serum were extrapolated in GraphPad Prism 9 using a standard curve that was generated with the appropriate purified isotype version of Sal4 or CAM003.

Bacterial whole cell ELISA

For STm whole cell ELISA (WCE), an overnight culture of STm (ATCC 14028s) was inoculated with one colony from a freshly streaked plate into 5mL of LB broth. The following day, the overnight STm culture was subcultured 1:50 in LB broth and grown to OD_{600} of 0.7–0.8, with a final adjusted concentration of OD_{600} 0.7. Cells were washed 2x with sterile PBS and resuspended in the prewash volume. NUNC MaxiSorp or Immulon 4HBX plates (Thermo Fisher Scientific) were coated with 0.1 mL per well of the STm bacterial solution, covered and incubated at 4°C overnight. For *P. aeruginosa* PA01 WCE, 10 to 50 mL of LB broth was inoculated with one colony from a freshly streaked plate. Bacteria were grown to an OD_{650} of ~2.0 and subsequently diluted with LB broth to an OD_{650} of 0.5, followed by an additional 50% dilution with sterile PBS. NUNC MaxiSorp plates were coated with 0.1 mL per well of the PA01 bacterial solution, covered and incubated at 4°C overnight. For STm WCE, wells were washed 4x with 0.5% PBS-T and blocked in either 0.2 mL of Superblock PBST (Thermo Fisher Scientific) or 2% goat serum in PBS-T for 2 h at room temperature. For PA01 WCE, wells were washed 4x with 0.5% PBST in an automated plate washer (Biotek) and subsequently blocked with 0.2mL Superblock PBST (ThermoFisher) for 2 h at room temperature. Subsequent ELISA steps are identical to what has been described previously.

HeLa cell invasion assay

HeLa cells were obtained from the ATCC and maintained in Dulbecco's Modified Eagle Media (DMEM) with 10% fetal bovine serum at 37°C and 5% CO_2. The HeLa cell invasion assay was performed as described.[25] Cells were seeded at $5x10^5$ cells/mL in 96-well plates and grown for 24 h until 70%–90% confluent. Prior to invasion assays, cells were washed 3x with serum-free DMEM. Overnight cultures of GGW444 (O5+) and GGW445 (O5-) were diluted 1:50 into LB at 37°C and 220 rpm and adjusted to an OD_{600} of 0.7. Strains were mixed 1:1 and washed 2x by centrifugation (6,000 x *g* for 4 min) and resuspended in PBS with a pH of 7.4. Bacteria were diluted 1:10 in Hanks' Balanced Salt Solution (HBSS, Sigma-Aldrich); an aliquot was plated on LB agar supplemented with kanamycin (100 μg/mL) and X-gal (40 μg/mL) for subsequent determination of CFUs associated with bacterial input.

For the invasion assay, bacterial mixtures were incubated with 15 μg/mL of Sal4 IgA for 15 min at 37°C. The source of Sal4 IgA used in these studies was either recombinant purified protein (GeneArt) or concentrated supernatant 2 days following transfection of EXPI-293 with Sal4 IgA_{mRNA}. Treated bacteria were applied to HeLa cell monolayers and the culture plate was centrifuged at 1,000 x g for 10 min. The microtiter plates were then incubated for 60 min at 37°C and the cells washed 3x with HBSS and treated with gentamicin

(100 μg/mL) to eliminate extracellular bacteria. Cells were then washed 3 times with HBSS and lysed with 1% Triton X-100 (in Ca^{2+} and Mg^{2+}-free PBS)., The cells were then serially diluted and plated on LB agar containing kanamycin (100 μg/mL) and X-gal (40 μg/mL), and then incubated overnight at 37°C. The competitive index (CI) [(%strain A recovered/% B strain recovered)/(%strain A inoculated/% strain B inoculated)] was calculated for each treatment group.

Purification of Sal4 IgA

Purification proceeded identically for both mRNA and DNA transfections. To harvest, suspension cultures were centrifuged at 4,000 rcf for 30 min and pellets were discarded. Cell supernatant was filtered through a 0.22 μm vacuum filter followed by gravity chromatography with columns packed with CaptureSelect IgA Affinity Matrix (ThermoFisher). Columns were washed with PBS before eluting in 0.1 M Glycine pH 3 and were then immediately neutralized with 1 M Tris with a pH of 8. Affinity purified IgA was then injected onto a Superdex 200 Increase 10/300 GL gel filtration column (Cytiva) using an AKTA Pure FPLC.

SDS-PAGE

For SDS-PAGE analysis, 20 μL of SEC fractions were mixed with 4X Laemmli Sample Buffer (Bio-Rad). Reducing conditions were achieved with 5% (v/v) 2-mercaptoethanol in sample buffer. Samples were heated to 95°C for 5 min prior to loading onto 4–20% Mini-Protean TGX Stain-Free gel (Bio-Rad), with Precision Plus Protein Unstained Protein Standards included as marker (Bio-Rad). Gels were run for 30 min at 200 V in Tris-Glycine-SDS running buffer (Invitrogen), the stain-free dye was developed via UV activation and then imaged on ChemiDoc MP gel imager (Bio-Rad).

Transmission electron microscopy (TEM) imaging

For each sample, a ~3.5 μL aliquot was applied to a freshly glow-discharged, carbon-coated copper grid (Electron Microscopy Sciences, CF300-Cu) and allowed to absorb for 30 s. After blotting the excess solution, grids were stained with 1% uranyl acetate solution (Electron Microscopy Sciences) for 1 min and then air-dried. A Thermo Fisher Scientific Talos L120C electron microscope equipped with a 4k x 4k Ceta CMOS Camera was used for data collection. Images were captured at a nominal magnification of 57,000× and 73,000x (pixel size 2.60 Å/pixel and 2.04 Å/pixel, respectively) with a defocus range of ~ −1.5 to −2 μm.

Expression of mAbs in mice

Six-to 8-week-old female BALB/c mice (Charles River Laboratories), in groups of 5–28 mice each, were injected intravenously with the indicated recombinant protein, mRNA/LNP, or PBS, at the indicated dose in 100 μL. All *in vivo* studies with mRNA/LNP were co-formulations of HC and LC for IgG and HC, LC, and JC for IgA. For IgA, this results in a mixture of monomeric, dimeric, and polymeric IgA. Unless otherwise stated, all IgA_R injected into mice is a mixture of monomeric, dimeric, and polymeric. At the doses used major adverse reactions, pathology or mortality was not observed or linked to mRNA/LNP treatment in animals. Mice were bled via submandibular vein at the indicated time points and serum was isolated for antibody quantification by ELISA. At the final indicated time point, mice were euthanized via CO_2 asphyxiation and a terminal bleed was collected via cardiac puncture.

Mouse tissue processing for mAb quantification

For fecal samples, three to four fresh fecal pellets were collected at each of the indicated time points following intravenous administration of test articles. Total weight of the fecal pellets per mouse were recorded and fecal extract buffer (PBS containing 10% normal goat serum [Gibco] and 1 protease inhibitor per 50mL solution [Pierce A32953]) was added to achieve a final concentration of 200 mg/mL. Pellets were vortexed and manually broken until the entire pellet was disrupted. Following centrifugation at 13,000 rpm for 10 min at 4°C, supernatants were collected and mAb concentrations were quantified via ELISA.

Where indicated, intestines were harvested at 168 h after injection following CO_2 asphyxiation and washed in PBS to remove any mucous or fecal debris. Each mouse intestine (comprising both the small and large intestine) was weighed and homogenized (2x at 5 m/s for 45 s, with a 10 s break between sets) at 2 g/mL in homogenization buffer (PBS +10% normal goat serum) in 2.0 mL homogenizing tubes containing 2.8 mm ceramic beads (Fisherbrand) using the BeadMill homogenizer (Fisherbrand). Eppendorf tubes containing homogenized intestinal tissue were spun at 13,000 rpm for 10 h at 4°C to obtain debris-free supernatant which was stored for further analysis by ELISA.

Purification of IgA2 from mouse serum

Fifty Balb/c mice per group (8–10 weeks old; Charles River Laboratory) were intravenously administered either 1 mg/kg of the indicated mRNA/LNP formulations or PBS and terminal bleed serum was collected 24 h following administration (Figure S2). At this dose, major adverse reactions, pathology or mortality was not observed or linked to mRNA/LNP treatment in animals. Sal4 IgA2 was purified from pooled mouse sera using peptide M agarose (Invivogen) following the manufacturer's instructions. Briefly, the sera were concentrated by 100kDa Pierce Protein Concentrators PES (Thermo Fisher), then buffer exchanged with PBS buffer. The sera whereas then incubated with peptide M agarose resin overnight at 4°C, and the resin was washed using PBS buffer. After another wash step with 0.1 M glycine buffer (pH 5.0), IgA2 was eluted with 0.2 M glycine buffer (pH 2.5) and incubated for 5 min at room temperature. The elution step was repeated 3x, and the eluted IgA2 concentration of the administered group and control group were measured by ELISA.

Isolation of recombinant IgA2 monomer

Sal4 IgA2 expressed by EXPI293 cell line as described above was further using the AKTA pure protein purification system. The monomeric IgA2 ($_{m}IgA2_{R}$) was isolated for glycosylation comparison with mRNA expressed IgA2 *in vivo* (Figure S2). Briefly, 1mg of the total IgA2 was injected to Superdex 200 Increase 10/300 GL column (Cytiva) and then IgA2 was eluted by PBS buffer at a constant flow rate of 0.25 mL/min. The eluent was collected by AKTA fraction collector F9-C (0.5 mL per fraction). The fractions of monomer were determined using Western blot and combined for the next step of the experiment.

Protein digestion

Sal4 IgA2 proteins from different sources were concentrated to 20 μL by 100 kDa Pierce Protein Concentrators PES, then buffer exchanged with UA buffer (8 M urea in 50 mM Tris-HCl buffer pH 7.8). Dithiothreitol (Sigma-Aldrich) was added to the solution to a concentration of 10 mM; the solution was then heated at 95°C for 10 min. Once cooled to room temperature, iodoacetamide (Sigma-Aldrich) was added to the solution to a concentration of 20 mM. The solution was then incubated in darkness at room temperature for 40 min and another 10 mM dithiothreitol was added to quench the reaction. The solution was then diluted with 200 μL of 0.5 mM Glu-Glu (Sigma-Aldrich) in 50 mM Tris-HCl buffer at a pH of 7.8. Endoproteinase GluC (New England Biolabs) was added to make GluC and IgA2 at a 1:10 ratio (w/w), and the solution was incubated at 37°C overnight. The sample was further digested with Trypsin to a final protease:protein ratio of 1:50 (w/w) for 4 h at 37°C. The reaction was quenched by adding 0.1% Formic Acid (Fisher Scientific) and the digested peptides were desalted using HyperSep C18 Cartridges (Fisher Scientific). The desalted peptides were then dried by Savant SpeedVac Concentrator (Thermo Fisher Scientific) and stored at −80°C.

N-glycosylation site analysis

N-linked glycosylation sites of Sal4 IgA2 were de-glycosylated and labeled with ^{18}O using a previously reported method (Figure S2).[49] Sal4 IgA2 proteins from different sources were dissolved in 30 μL of 20 mM ammonium bicarbonate (Sigma-Aldrich) in $H_2{}^{18}O$. One unit of PNGase F (Sigma-Aldrich) was then added, and the solution was incubated for 1 h at 37°C to label the *N*-glycosylation sites. The solution was stored at −80°C for mass spectrometry analysis (Figure S2).

Glycopeptide enrichment

N-linked intact glycopeptides of Sal4 IgA2 were enriched by HILIC using a previously reported method.[50] ZIC-HILIC particles (The Nest Group, Inc.) were packed in C4 HyperSep tips (Thermo Fisher Scientific). The HILIC tip was then conditioned 3x in LC-MS grade water (Fisher Scientific) followed by conditioning (3x) in 1 mL of 80% acetonitrile (ACN), 0.1% trifluoroacetic acid (TFA). Sal4 IgA2 proteins from different sources were dissolved 3x in 80% ACN and 0.1%TFA and loaded onto HILIC tips. The HILIC tips were then washed 3x with 80% ACN and 0.1%TFA, and the glycopeptides were eluted 3x using 100% water, 0.1%TFA. The eluent was dried by lyophilizer (Labconco) and store at −80°C for mass spectrometry analysis (Figure S2).

Mass spectrometry analysis

Peptides or glycopeptides were dissolved in different volumes of 0.1% formic acid (FA) and separated (in three technical executions) through a Waters ACQUITY UPLC M-Class liquid chromatography system equipped with an Easy-Spray PepMap *Neo* C18 75 μm × 500 mm column (Thermo Fisher Scientific) coupled to a 20-mm nanoEase C18 Trap Column trap column (Water Corporation). The mobile phase flow rate was 0.3 μL/min with 0.1% FA in water (A) and 0.1% FA 100% acetonitrile (B). The gradient profile was set as the following: 1%–35% B for 80 min, 35%–60% B for 10 min, 60%–95% B for 10 min, 95% B for 5 min, and equilibrated in 1% B for 10 min. MS analysis was performed using a Thermo Orbitrap Fusion mass spectrometer (Thermo Fisher Scientific). The spray voltage was set at 1.9 kV. Spectra (maximum IT of 100 ms) were collected from 400 to 2000 m/z at a resolution of 120 K followed by data-dependent HCD MS/MS (at a resolution of 6K, stepped NCE 20,30,40, intensity threshold of 1×10^5 and maximum IT of 100 ms) of the 20 most abundant ions using an isolation window of 2 m/z. Charge-state screening was set to only include ions with more than one and less than eight charges.

Data analysis

N-glycosylation sites data from the ^{18}O label experiment was processed with Proteome Discoverer 2.5 (Thermo Fisher Scientific). Glycopeptides were identified by Byonic software (Protein Metrics Inc.). The LC-MS/MS spectra of combined GluC/tryptic digests of glycoproteins were searched against the FASTA sequence of Sal4 IgA2 by choosing RKDE as cleavage sites with a maximum of two missed cleavage sites. MS/MS spectra were matched with a tolerance of 10 ppm on precursor mass and 50 ppm on a fragment mass. All protein identification hits had an FDR rate $\leq$1%. Carbamidomethylation was set as fixed modification, oxidation of methionine, and deamidation of asparagine and glutamine were used as variable modifications. In Proteome Discoverer, ^{18}O labeling of Asn ($\Delta m = 2.9848$) was set as variable modification to determine *N*-glycosylation sites and *N*-glycan occupancy (Figure S2). Intact-glycopeptide data were searched against the common mammalian *N*-glycans database in Byonic. Glycans were manually categorized according to their composition using the following criteria: HexNAc(2)Hex(9−4) was classified as high-mannose. HexNAc(3)Hex(5−6)X was classified as hybrid (X can be fucose or sialic acid). Other compositions were classified as complex-type glycans. If any of the compositions had a fucose, it was assigned as a fucosylated glycan. Any glycan containing at least one sialic acid was counted as sialylated.[51] Glycopeptides with more than five MS/MS spectral identified (PSM#) were used for quantifying the

percentage of glycans belonging to any of the three categories, which include complex, hybrid, or high-mannose (Figure S2).[52] The same method was used to determine the percentage of fucosylation and sialylation among all glycans. IgA2 was undetectable in both HILIC-enriched and ^{18}O-labeled aliquots of the serum pool from PBS-administered animals.

STm intragastric challenge

Four mice per group of female Balb/c mice aged 8 to 12 weeks (Taconic Biosciences) were used for each challenge and the challenge was repeated four separate times (16 mice in total per group). The challenge experiments were performed as previously described with some modifications.[25] This model utilizes a competitive infection assay to normalize natural variations in challenge inoculum using two STm strains premixed prior to oral delivery: one expressing the Sal4 epitope, the O5 antigen (O5+), and an O5-null strain (O5-) that expresses β-galactosidase to easily distinguish the two strains. A reduction in competitive index (CI) only occurs when Sal4 reduces the number of O5+ in mouse Peyer's patches.

Briefly, mice were injected intravenously with saline, 1 mg/kg of formulated mRNA modified with 3′idT, or 5 mg/kg of recombinant protein, 24 h prior to bacterial challenge. At the doses used major adverse reactions, pathology or mortality was not observed or linked to mRNA-LNP treatment in the animals. Overnight cultures of GGW444 (O5+) and GGW445 (O5-) were subcultured to an OD_{600} of 0.7, combined 1:1 (v/v) and resuspended in sterile PBS pH 7.4. Following this, an aliquot was plated on LB agar containing kanamycin (100 μg/mL) and X-gal (40 μg/mL) at the start of the experiment. Mice were given an STm gavage (~4x10^7 CFUs in 200 μLs) and sacrificed (CO_2 asphyxiation followed by cervical dislocation) 24 h after challenge, following which the small intestine was removed above the cecum for each mouse. The Peyer's Patches from each mouse were then pooled in 1 mL sterile PBS and placed on ice. Samples were then homogenized 3x for 30 s each using a Bead Mill 4 Homogenizer (Fisher Scientific) and the homogenates serially diluted and plated on LB agar (containing 100 μg/mL kanamycin and 40 μg/mL X-gal) and incubated overnight at 37°C. The number of blue and white colonies were determined and the competitive index (CI) was calculated as [(%strain A recovered/% B strain recovered)/(%strain A inoculated/% strain B inoculated)]. Whole plate dilutions at 100 μL per plate were required in order to observe the required number of colonies to calculate CI. Samples containing fewer than 30 CFUs/100 μL were removed and considered "too few to count".

P. aeruginosa lethal acute pneumonia mouse model

Female Balb/c mice (22 ± 2g) (Envigo Laboratories), 6–8 weeks old, were administered the indicated dose of mRNA/LNP formulations or recombinant protein intravenously (n = 8–10/group) and serum was collected 24 h later to quantitate circulating antibody titers prior to challenge. At the doses used major adverse reactions, pathology or mortality was not observed or linked to mRNA-LNP treatment in the animals. Mice were subsequently challenged intranasally with *P. aeruginosa* PAO1 and monitored for mortality for 6 days. Results were graphed in a Kaplan-Meier survival curve.

QUANTIFICATION AND STATISTICAL ANALYSIS

Data was processed using GraphPad Prism 9 and unless otherwise stated, all statistical analysis was performed in this software. Mean and standard deviation are presented as averages and error bars. *In vitro* tests were performed in triplicate and either averaged or a single representative experiment was shown. Where applicable, Student's T test was used to analyze the statistical differences between independent groups in *in vitro* experiments. Unless otherwise stated, all *in vivo* experiments comprised of 5–28 mice per group. For STm intragastric challenge, four mice per group were used and the challenge was repeated four separate times. Statistical significance was determined by a Kruskal-Wallis test and Dunn's post hoc test. Kaplan-Meier survival curves were utilized for the *P. aeruginosa* acute pneumonia challenge model and differences in survival were calculated by the log rank test for IgA1 versus IgG1. All differences were considered significant when p values were less than 0.05 and significance is denoted by asterisks (*p < 0.05, **p < 0.01, and ***p < 0.001).

For EM images, reference-free 2D classification was performed using Relion 4.0 software. Glycosylation data analysis was performed using Proteome Discoverer 2.5 (Thermo Fisher Scientific) to process the N-glycosylation sites data from the ^{18}O label experiment. Additionally, glycopeptides were identified by the Byonic Software (Protein Metrics Inc)

Statistical model for IgA half-life modeling

Since each analyte was measured at different time points, we fit the following model to each analyte separately. We estimated the population-level half-life of each analyte using a flexible linear mixed effects model that incorporates a first-order kinetic component for terminal measurements. To do so, we modeled the terminal decay phase of the data using a first-order kinetic model but employed a flexible spline basis to model the earlier phases. Let y_{ij} be the measured analyte concentration for animal i at time t_{ij}, where $i = 1, \ldots, n$ and $t_{ij} = t_{i1}, \ldots, t_{in_i}$. To treat the early and terminal phase of the time course differently, we introduce variables x^0_{ij} and x^1_{ij}, defined as

$$x^0_{ij} = \begin{cases} t_{ij} & t_{ij} \le t \\ 0 & t_{ij} > t \end{cases} x^1_{ij} = \begin{cases} 0 & t_{ij} \le t \\ t_{ij} & t_{ij} > t \end{cases} \quad \text{(Equation 1)}$$

where t is some fixed threshold after which the terminal decay phase has begun. Then,

$$log(y_{ij}) = \begin{cases} \beta_0 + \beta_1 x_{ij}^1 + f\left(x_{ij}^0\right) + \gamma_{0i} + \gamma_{1i} x_{ij}^1 + \epsilon(t_{ij}) & y_{ij}^\star \geq L \\ log(L) & y_{ij}^\star < L \end{cases} \quad \text{(Equation 2)}$$

where $y_{ij}^\star$ is the concentration of the analyte for animal i at time t_{ij} prior to censoring by the lower limit of quantification (LLOQ), L is the LLOQ of the assay, t is a threshold after which the decay process has entered the terminal phase, and f is a k-dimensional thin plate regression spline basis.[53]

We allow for animal-specific random intercepts and slopes, where the random slopes imply animal-specific deviations about the population-level terminal IgA half-life. Therefore, we have

$$\gamma_i = \begin{pmatrix} \gamma_{0i} \\ \gamma_{1i} \end{pmatrix} \overset{\text{iid}}{\sim} N\left(\begin{pmatrix} 0 \\ 0 \end{pmatrix}, \begin{pmatrix} \tau_0^2 & 0 \\ 0 & \tau_1^2 \end{pmatrix} \right) \quad \text{(Equation 3)}$$

We allow residual variance to change with time following a 7-dimensional thin plate spline regression basis, giving $\epsilon(t_{ij}) \sim N(0, \sigma_{t_{ij}}^2)$.

In order to choose the threshold t, for each analyte, we selected the latest t to allow for ≥ 3 time points where the majority of measurements were above the LLOQ. Since all $IgA2_R$ measurements were above the LLOQ, we selected the t such that the last 3 time points were used to estimate the terminal half-life. For $IgA2_{mRNA}$ and human serum IgA, the last 4 time points were used to estimate terminal half-life. The dimension of the thin plate regression spline basis f was chosen to be as large as possible, given the threshold t.

All modeling was implemented using the R package brms (version 2.17.3)[54] using default, non- or weakly-informative prior specifications.